RESEARCH ARTICLE | MAGNETISM AND MAGNETIC MATERIALS | MARCH 01 2016

Core/shell-structured nickel/nitrogen-doped onion-like carbon nanocapsules with improved electromagnetic wave absorption properties

Niandu Wu; Xianguo Liu; Siu Wing Or

AIP Advances 6, 056206 (2016)
https://doi.org/10.1063/1.4943357

Core/shell-structured nickel/nitrogen-doped onion-like carbon nanocapsules with improved electromagnetic wave absorption properties

Niandu Wu,[1,2] Xianguo Liu,[1,2] and Siu Wing Or[2,a]
[1]*School of Materials Science and Engineering, Anhui University of Technology, Maanshan 243002, PR China*
[2]*Department of Electrical Engineering, The Hong Kong Polytechnic University, Hung Hom, Kowloon, Hong Kong*

(Presented 13 January 2016; received 4 November 2015; accepted 16 December 2015; published online 1 March 2016)

Core/shell-structured nickel/nitrogen-doped onion-like carbon (Ni/(C, N)) nanocapsules are synthesized by a modified arc-discharge method using N_2 gas as the source of N atoms. Core/shell-structured Ni/C nanocapsules are also prepared for comparison. The Ni/(C, N) nanocapsules with diameters of 10–80 nm exhibit a clear core/shell structure. The doping of N atoms introduces more lattice defects into the (C, N) shells and creates more disorderly C in the (C, N) shells. This leads to a slight shift in the dielectric resonance peak to the lower frequency side and an increase in the dielectric loss tangent for the Ni/(C, N) nanocapsules in comparison with the Ni/C nanocapsules. The magnetic permeability of both types of nanocapsules remains almost unaltered since the N atoms exist only in the (C, N) shells. The reflection loss (*RL*) of the Ni/(C, N) nanocapsules not only reaches a high value of -35 dB at 13.6 GHz, but also is generally improved in the low-frequency S and C microwave bands covering 2–8 GHz as a result of the N-doping-induced additional dipolar polarization and dielectric loss from the (C, N) shells.
[http://dx.doi.org/10.1063/1.4943357]

I. INTRODUCTION

Core/shell-structured nanocapsules composed of a magnetic nanoparticle core and a dielectric shell of nanometer size offer a promising strategy for realizing next generation electromagnetic (EM) wave absorbers.[1–3] Specifically, the steady permeability and high Snoek's limit in the gigahertz frequency range enabled by the magnetic cores as well as the high permittivity and good oxidation and corrosion protections empowered by the dielectric shells generally result in physically interesting complementary effects for absorbing EM waves. The major deficiencies of the reported nanocapsules involve strong absorptions in limited frequency ranges and large variations in absorption with absorber thickness.

Core/shell/shell-structured nanocapsules are recently proposed to extend the absorbing bandwidth and absorber thickness range by inducing multidielectric polarizations in the double-shell.[4–6] Recalling that doping with foreign atoms is a useful method to modify material properties. Nitrogen (N)-doping can manipulate surface chemistry, alter lattice alignment or structural properties, and give rise to obvious changes in materials properties.[7,8] Today, there does not appear to be any work reporting the EM wave absorption properties of N-doped nanocapsules. Among various types of nanocapsules, the one based on nickel/carbon (Ni/C) is regarded as an important candidate because

[a]Author to whom correspondence should be addressed: electronic mail: eeswor@polyu.edu.hk

of its better EM impedance match between the magnetic and dielectric components, lighter weight, higher environmental stability, and lower cost.[1–3]

In this work, we aim to study the effect of doping, specifically N-doping, on the EM wave absorption properties of Ni/C nanocapsules. Accordingly, Ni/(C, N) nanocapsules with Ni nanoparticles as the core and N-doped onion-like C as the shell are synthesized using a modified arc-discharge method with N_2 gas as the N atom source. The microstructure and EM wave absorption properties of the Ni/(C, N) nanocapsules are investigated, together with the Ni/C nanocapsules. In fact, the use of onion-like C shell is to provide a larger space for preventing the Ni core from volume swing and hence pulverization as well as aggregation on the basis of its defective morphology.[9,10]

II. EXPERIMENTS

A modified arc-discharge method using N_2 gas as the N atom source was used to synthesize the proposed Ni/(C, N) nanocapsules. A Ni ingot of 99.9% purity was placed in a water-cooled Cu crucible as the anode, while a graphite rod was employed as the cathode. The arc-discharge chamber was evacuated to 10 mPa and an Ar/H_2 gas mixture of 4:1 was introduced into the chamber as the plasma source. Meanwhile, N_2 gas of 15 kPa and ethanol of 20 ml were added into the chamber as the N and C sources, respectively. An arc-discharge current of 80 A was applied to the chamber for 1 h to ensure a sufficient evaporation of the Ni ingot. The Ni/(C, N) product of ~4.5 g was collected from the inner surface of the chamber after it was passivated in N_2 gas for 10 h. For comparison, Ni/C nanocapsules were also synthesized under the same condition but in the absence of N_2 gas.

The phase analysis of the Ni/(C, N) and Ni/C products was performed by an X-ray diffractometer (XRD, Brucker D8 Advance) with Cu-K_α radiation (λ=1.54 Å). The valence of N atoms of the shells was evaluated by an X-ray photoelectron spectroscope (XPS, ESCALAB-250) with a monochromatic X-ray source (an Al-K_α line of 1486.6 eV energy and 150 W) at a depth of 1 nm. The morphology and microstructure were analyzed by a transmission electron microscope (TEM, JEOL 2010) at an emission voltage of 200 kV. The C state of the shells was characterized using Raman spectroscope (Renishaw 2000) with a 514.5 nm wavelength argon ion laser. The as-prepared nanocapsules were mixed with 60 wt.%, EM wave-transparent paraffin to form composite samples of different thicknesses (d) of 2.0–9.5 mm for the subsequent measurements of their complex relative permittivity ($\varepsilon_r = \varepsilon_r' - j\varepsilon_r''$) and permeability ($\mu_r = \mu_r' - j\mu_r''$) by a transmission/reflection coaxial line method in the 2–18 GHz range using a vector network analyzer (Anritsu 37269D). The frequency (f) dependence of reflection loss (RL) was determined using[11]

$$RL = 20\log|(Z_{in} - Z_0)/(Z_{in} + Z_0)| \quad (1)$$

where $Z_{in} = Z_0(\mu_r/\varepsilon_r)^{1/2}\tanh\left[j(2\pi f d/c)(\mu_r\varepsilon_r)^{1/2}\right]$ is the input impedance of composite sample, Z_0~377 Ω is the characteristic impedance of air, $c = 3 \times 10^8$ m/s is the velocity of light, and d is the thickness of composite sample.

III. RESULTS AND DISCUSSION

Figure 1(a) shows the XRD pattern of a typical Ni/(C, N) product. All diffraction peaks with 2θ values of 44.5°, 51.9°, and 76.4° can be assigned to the (111), (200), and (220) planes of fcc-Ni, indicating that Ni is the major phase of the Ni/(C, N) product. No clear peaks in relation to carbon, carbide or nitride are detected due to their small amounts or amorphous state, if any. Figure 1(b) plots the XPS spectrum of N 1s for the Ni/(C, N) product. The largest peak detected at 403.9 eV binding energy can be attributed to N_2 gas, while the two smaller peaks found at 402.4 and 406.0 eV correspond to N–C compounds.[12–14] The observation suggests that N atoms are in contract with C atoms in the (C, N) shells and mainly appear as N_2 on the surface of the product. From the full XPS spectra (not shown), the atomic percentage of N doping in the Ni/(C, N) product is found to be 1.24 at.%. Figure 1(c) illustrates the TEM image of the Ni/(C, N) product. It is clear that the Ni/(C, N) product is spherical in shape with a diameter of 10–80 nm. These spherical nanoparticles agglomerate loosely because of their small dimensions and high surface energy.

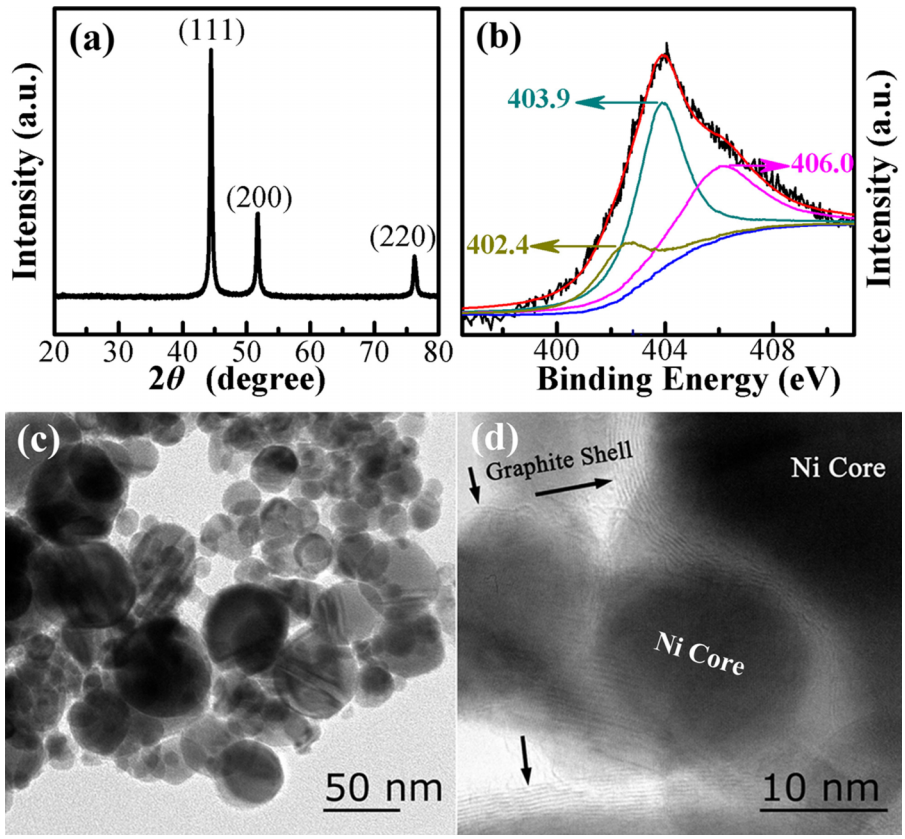

FIG. 1. (a) XRD pattern, (b) XPS spectrum of N 1s, (c) TEM image, and (d) HRTEM images of a typical Ni/(C, N) product.

Figure 1(d) displays the HRTEM image of the spherical nanoparticles in Fig. 1(c). It is seen that the nanoparticle cores are encapsulated by onion-like shells of 1–4 nm thickness and the core/shell interface is distinct. The variation of onion-like shell thickness has no obvious correlation with the nanoparticle core size based on statistical approach. The lattice plane spacing of the onion-like shells is ~0.34 nm, corresponding to the *d*-spacing of (002) planes of the bulk graphite. Moreover, the masses of lattice imperfections, including collapses, dislocations, and bending, can be observed at the (C, N) shells. The defective morphology is capable of providing a larger space to prevent the Ni core from volume swing and hence pulverization as well as aggregation.[9,10]

Figure 2 shows the Raman spectra of the Ni/(C, N) and Ni/C nanocapsules. Two main peaks are observed in the Raman shift range of 1000–2000 cm^{-1}. The first peak at ~1315 cm^{-1} (marked as D peak) originates from the in-plane symmetric C-C stretching vibrations governed by the symmetry breaking phenomena, while the second peak at ~1596 cm^{-1} (marked as G peak) results from the stretching vibrations of any C pairs of sp^2 sites.[2] Both types of nanocapsules exhibit strong D peaks, indicating the presence of a large number of lattice defects in their shells and confirming the observations in the HRTEM image in Fig. 1(d). The stronger D peak in the Ni/(C, N) nanocapsules compared to the Ni/C nanocapsules implies the existence of more disorderly C in the (C, N) shells. The intensity ratio of D peak to G peak (I_D/I_G) is generally used to describe the extent of graphitization.[15] The I_D/I_G ratio of the Ni/(C, N) nanocapsules is ~1.21, which is larger than the Ni/C nanocapsules of ~1.06. This supports our proposal on inducing more disorderly C in the (C, N) shells by introducing additional lattice defects/imperfections into them through the doping of N atoms.

Figures 3(a) and 3(b) plot the f dependence of ε_r' and ε_r'' of the paraffin-bonded Ni/(C, N) and Ni/C composite samples, respectively. ε_r' and ε_r'' represent the amount of polarization and the level of energy dissipation, respectively.[5,6] It is seen that ε_r' and ε_r'' of both types of composites

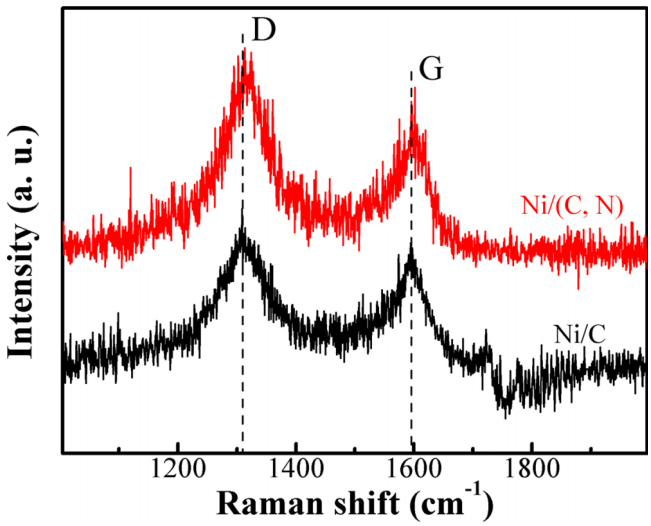

FIG. 2. Raman spectra of Ni/(C, N) and Ni/C nanocapsules.

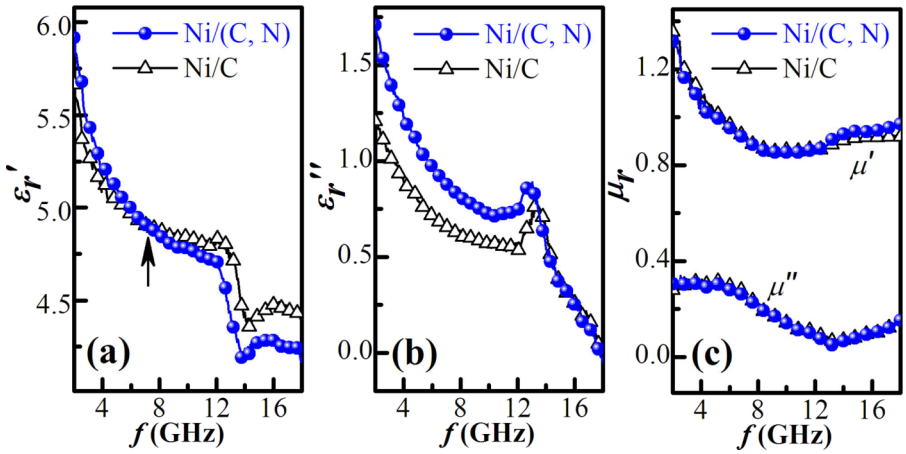

FIG. 3. f dependence of (a) ε_r' and (b) ε_r'' of paraffin-bonded Ni/(C, N) and Ni/C composites. (c) f dependence of μ_r' and μ_r'' of the composites.

demonstrate similar quantitative decreasing trends with increasing f in the 2–18 GHz, except for the dielectric resonance in the 12–14 GHz range. In Fig. 3(a), the Ni/(C, N) composite exhibits a more rapid decrease in ε_r' from 5.92 to 4.19 in comparison with the Ni/C composite of 5.58–4.41. Specifically, the Ni/(C, N) composite has larger ε_r' values in the 2–7.6 GHz range but smaller in the 7.6–18 GHz range. In Fig. 3(b), clear dielectric resource peaks at 12.7 and 13.5 GHz are observed for the Ni/(C, N) and Ni/C composites, respectively, as a result of the permanent electric dipoles caused by the defects in the shells.[16] It is noted that more free charges will be trapped by defects under EM fields, giving rise to a more obvious asymmetric charge distribution over the defects. Thus, the defective sites play the role of permanent dipolar polarization centers, leading to additional dielectric polarization.[17,18] The reason why the Ni/(C, N) composite displays a slight shift in the dielectric resonance peak to the lower frequency side with respect to the Ni/C composite is mainly due to the N-doping-induced additional dipolar polarization contribution in the (C, N) shell. ε_r'' is elevated in the Ni/(C, N) composite in the 2–14 GHz range in relation to the Ni/C composite because of the improved dielectric properties by the doping of N atoms. Figure 3(c) shows the f dependence of μ_r' and μ_r'' of the Ni/(C, N) and Ni/C composites. The almost unaltered permeability values between the two types of composites imply the same state of Ni core because the N atoms exist only in the shells.

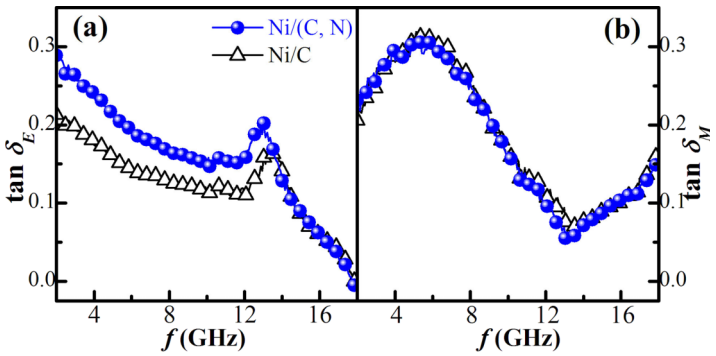

FIG. 4. f dependence of (a) tanδ_E and (b) tanδ_M of paraffin-bonded Ni/(C, N) and Ni/C composites.

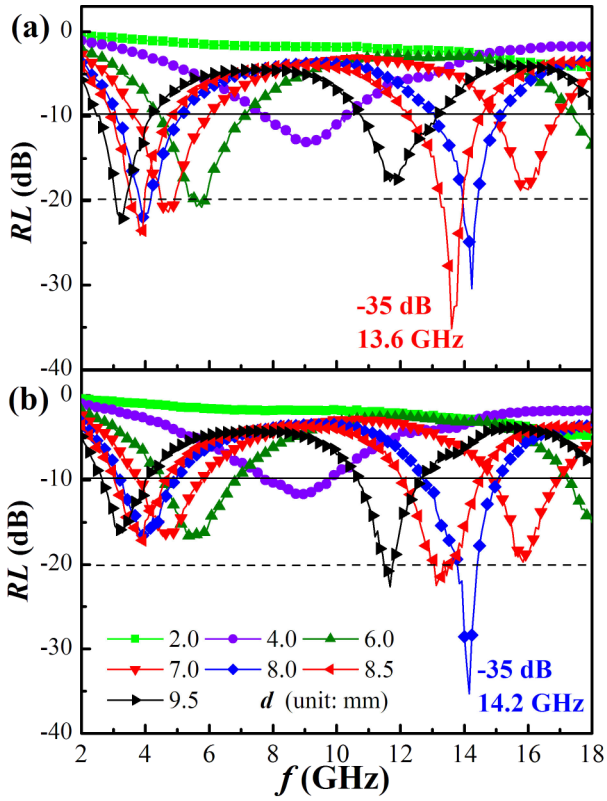

FIG. 5. *RL* spectra of the paraffin-bonded (a) Ni/(C, N) and (b) Ni/C composites at different d of 2.0–9.5 mm.

Figures 4(a) and 4(b) show the f dependence of the dielectric loss tangent (tan$\delta_E = \varepsilon_r''/\varepsilon_r'$) and magnetic loss tangent (tan$\delta_M = \mu_r''/\mu_r'$) of the Ni/(C, N) and Ni/C composites, respectively. The tanδ_E and tanδ_M values, which reflect the mechanism of losses of EM waves, are calculated from the ε_r', ε_r'', μ_r', and μ_r'' values in Fig. 3. The Ni/(C, N) composite has larger tanδ_E values than the Ni/C composite in the 2–14 GHz range owing to the creation of more disorderly C in the (C, N) shells. The curves of tanδ_M almost overlap with each other since the N-doping has no obvious effect on the magnetic properties.

Figure 5 shows the *RL* spectra of the Ni/(C, N) and Ni/C composites at different d of 2.0–9.5 mm. The *RL* values are determined in accordance with Eq. (1). By selecting an appropriate d, *RL* of both types of composites can reach -10 dB, which corresponds to 90% absorption, in the whole range of 2–18 GHz. In particular, the Ni/(C, N) and Ni/C composites can achieve the largest *RL* of -35 dB at 13.6 GHz for d = 8.5 mm and at 14.2 GHz for d = 8.0 nm, respectively. The

outstanding EM wave absorbability can be attributed to good EM complementarities between the dielectric and magnetic losses. It is important to note that the *RL* values of the Ni/(C, N) composite are generally improved in the low-frequency S and C microwave bands covering 2–8 GHz. Specifically, they exceed -20 dB, corresponding to 99% absorption, for frequencies as low as 3–6 GHz. By contrast, the Ni/C composite can only realize strong absorption at high frequencies above 11 GHz. This means that the Ni/(C, N) composite is capable of improving low-frequency absorption. The improvement is mainly due to the additional contribution of dipolar polarization and $\tan\delta_E$ enabled by the more disorderly C in the (C, N) shells through N doping. This is also to say that the modified arc-discharge method can provide a convenient way to adjust the atomic percentage of N doping, the amount of disorderly C, and hence the level of additional contribution of dipolar polarization and $\tan\delta_E$ in the Ni/(C, N) product via a control of the amount of N_2 gas added into the arc-discharge chamber.

IV. CONCLUSION

We have prepared core/shell-structured Ni/(C, N) and Ni/C nanocapsules and studied the effect of N-doping on the microstructure and EM wave absorption properties. The doping of N atoms in the C shells has been found to create more disorderly C in the (C, N) shells, resulting in additional dipolar polarization and dielectric loss contributions from the (C, N) shells compared to the undoped Ni/C shells. Therefore, the dielectric resonance peak and $\tan\delta_E$ of the Ni/(C, N) nanocapsules have undergone a down-shift from 13.5 to 12.7 GHz and an obvious increase in the 2–14 GHz range for the Ni/(C, N) nanocapsules with respect to the Ni/C nanocapsules. Moreover, *RL* of the Ni/(C, N) nanocapsules has exhibited a distinct improvement in the low-frequency S and C microwave bands covering 2–8 GHz, besides showing a similarly high value of -35 dB at 13.6 GHz. The N-doping has no observable effect on the magnetic properties because the N atoms exist only in the (C, N) shells rather than in the Ni core.

ACKNOWLEDGEMENTS

This work was supported by the Research Grants Council of the HKSAR Government (PolyU 5236/12E), The Hong Kong Polytechnic University (G-YK59), and the National Natural Science Foundation of China (51201002).

[1] X. F. Zhang, X. L. Dong, H. Huang, Y. Y. Liu, W. N. Wang, X. G. Zhu, B. Lv, and J. P. Lei, Appl. Phys. Lett. **89**, 053115 (2006).
[2] B. Lu, H. Huang, X. L. Dong, and J. P. Lei, J. Phys. D: Appl. Phys. **43**, 105403 (2010).
[3] H. Wang, H. H. Guo, Y. Y. Dai, D. Y. Geng, Z. Han, D. Li, T. Yang, S. Ma, W. Liu, and Z. D. Zhang, Appl. Phys. Lett. **101**, 083116 (2012).
[4] X. G. Liu, S. W. Or, S. L. Ho, C. C. Cheung, C. M. Leung, Z. Han, D. Y. Geng, and Z. D. Zhang, J. Alloys Compd. **509**, 9071 (2011).
[5] X. G. Liu, S. W. Or, C. M. Leung, and S. L. Ho, J. Appl. Phys. **115**, 17A507 (2014).
[6] J. H. Wang, S. W. Or, and C. M. Leung, J. Appl. Phys. **117**, 17A505 (2015).
[7] Y. Wang, Y. Y. Shao, D. W. Matson, J. H. Li, and Y. H. Lin, ACS Nano. **4**, 1790 (2010).
[8] D. L. Zhao, F. Luo, and W. C. Zhou, J. Alloy Compd. **490**, 190 (2010).
[9] X. G. Liu, S. W. Or, C. G. Jin, Y. H. Lv, C. Feng, and Y. P. Sun, Carbon **60**, 215 (2013).
[10] X. G. Liu, C. Y. Cui, N. D. Wu, S. W. Or, and N. N. Bi, Ceram. Inter. **41**, 7511 (2015).
[11] Y. Naito and K. Suetake, IEEE Trans. Microwave Theory and Tech. **19**, 65 (1971).
[12] H. Tillborg, A. Nilsson, B. Hernnas, N. Martensson, and R.E. Palmer, Surf. Sci. **295**, 1 (1993).
[13] S. Lalitha and P.T. Manoharan, J. Electron Spectrosc. Relat. Phenom. **49**, 61 (1989).
[14] K.D. Bartle, D.L. Perry, and S. Wallace, Fuel Process. Technol. **15**, 351 (1987).
[15] Z.S. Wu, W. Ren, L. Gao, J. Zhao, Z. Chen, B. Liu, D. Tang, B. Yu, C. Jiang, and H.M. Cheng, ACS Nano. **3**, 411 (2009).
[16] P. C. P. Watts, W. K. Hsu, A. Barnes, and B. Chambers, Adv Mater. **15**, 600 (2003).
[17] X. F. Zhang, P. F. Guan, and X. L. Dong, Appl. Phys. Lett. **96**, 223110 (2010).
[18] B. Lu, X. L. Dong, H. Huang, X. F. Zhang, X. G. Zhu, J. P. Lei, and J. P. Sun, J. Magn. Magn. Mater. **320**, 1106 (2008).